Original Article

Effect of *Agkistrodon acutus* venom (AAVC-I) on apoptosis through modulation of the Keap1/Nrf2 pathway in HSC-3 oral squamous cell carcinoma cells

Tao Tao[1,2#], Fang Zhang[1,3#], Lin Chai[1,2], Xin Xing[1,3], Chao Wan[1,3], Zhihao Tao[1], Zhiheng Wang[1,3]

[1]School of Stomatology, Wannan Medical College, Wuhu, China; [2]Anhui Provincial Engineering Research Center for Dental Materials and Application, Wannan Medical College, Wuhu, China; [3]Department of Oral and Maxillofacial Surgery, The First Affiliated Hospital of Wannan Medical College, Wuhu, China

Contributions: (I) Conception and design: T Tao, F Zhang; (II) Administrative support: Z Wang; (III) Provision of study materials or patients: X Xing, Z Tao; (IV) Collection and assembly of data: T Tao, Z Tao; (V) Data analysis and interpretation: T Tao, Z Tao; (VI) Manuscript writing: All authors; (VII) Final approval of manuscript: All authors.

[#]These authors contributed equally to this work.

Correspondence to: Zhiheng Wang, MM. Department of Oral and Maxillofacial Surgery, The First Affiliated Hospital of Wannan Medical College, No. 2 Zheshan West Road, Wuhu 241000, China; School of Stomatology, Wannan Medical College, Wuhu 241000, China. Email: 20111040@wnmc.edu.cn.

Background: Oral squamous cell carcinoma (OSCC) is the most common malignant tumor in the oral and maxillofacial regions. Patients with OSCC exhibit a poor response to conventional chemoradiotherapies, which are associated with severe side effects. Therefore, it is essential to identify an effective therapeutic method to treat patients with OSCC. An anti-tumor compound, *Agkistrodon acutus* venom component I (AAVC-I), purified from *Agkistrodon acutus* venom, has demonstrated anticancer activity both *in vitro* and *in vivo*. However, the mechanism of AAVC-I's anticancer activity in cancer cells has yet to be established. This study aimed to investigate the mechanism of AAVC-I-induced apoptosis in HSC-3 OSCC cells and explore its regulatory effect on oxidative stress.

Methods: Survival rates of human OSCC cell HSC-3 were detected by Cell Counting Kit-8 (CCK-8). The reactive oxygen species (ROS) level was analyzed by flow cytometry and fluorescence microscopy. The mitochondrial membrane potential was analyzed by cytometry and fluorescent microplate reader. Apoptosis of HSC-3 cells was analyzed using flow cytometry. The oxidative stress level was evaluated using glutathione (GSH), superoxide dismutase (SOD), and malondialdehyde (MDA) kits. In addition, the target proteins were analyzed by western blot.

Results: AAVC-I reduced HSC-3 cells' survival rates in a dose-dependent manner with a 50% inhibiting concentration (IC_{50}) of 8.86 μg/mL. It induced apoptosis of HSC-3 cells and the expression of cleaved caspase-3, cleaved caspase-9, and Cyt-c increased significantly, whereas the expression level of Bcl-2 decreased in AAVC-I-treated HSC-3 cells. Thus, AAVC-I caused apoptosis of HSC-3 via the activation of the intrinsic apoptotic pathway. In addition, AAVC-I reduced the mitochondrial membrane potential in HSC-3, enhanced intracellular ROS, and increased intracellular oxidative stress levels in comparison to that of untreated control cells. Furthermore, AAVC-I increased the expression of Kelch-like ECH-associated protein 1/nuclear factor erythroid 2-related factor 2 (Keap1/Nrf2) levels.

Conclusions: These findings demonstrate the inhibitory effects and associated mechanisms of AAVC-I on the HSC-3 OSCC cell line. This insight could be valuable for investigating AAVC-I as a potential therapeutic option for patients with OSCC.

Keywords: Snake venom; oral squamous cell carcinoma (OSCC); apoptosis; oxidative stress

Submitted Jan 26, 2024. Accepted for publication Jun 04, 2024. Published online Aug 17, 2024.
doi: 10.21037/tcr-24-182
View this article at: https://dx.doi.org/10.21037/tcr-24-182

Introduction

Oral squamous cell carcinoma (OSCC) is the most common malignant tumor in the oral and maxillofacial regions, accounting for more than 300,000 new cases worldwide each year. The prognosis of the disease is poor, with a 5-year survival rate of only 50–60%, despite significant efforts to improve clinical outcomes for patients with OSCCs (1-3). Patients with early-stage oral cancer are treated with a comprehensive series of surgeries. Those with advanced localized cancer require preoperative induction chemotherapy, whereas patients who cannot tolerate surgery are treated with chemoradiotherapies. However, the use of chemoradiotherapies can cause a number of adverse effects, including liver and kidney damage, bone marrow suppression, and so on, thus deteriorating the quality of life of the patients (4). Therefore, there is an urgent need to identify effective treatment options for patients with OSCCs.

Snake venoms are complex mixtures of toxins, containing a variety of active ingredients such as proteins, peptides, enzymes, and other bioactive substances with diverse biological activities (5,6). For example, *Agkistrodon acutus* venom component I (AAVC-I), an anti-tumor compound, is purified from the crude venom of *Agkistrodon acutus*. AAVC-I can inhibit proliferation by inducing apoptosis in various tumor cells, including lung and laryngeal cancer (7-9). However, its mechanisms of action have yet to be identified.

Oxidative stress is the imbalance between the production and consumption of reactive oxygen species (ROS), which plays crucial roles in the pathogenesis and progression of various cancers (10). Kelch-like ECH-associated protein 1/nuclear factor erythroid 2-related factor 2 (Keap1/Nrf2) signaling is the main regulatory pathway for cancer cells to resist ROS generation and protection against its harmful effects. Sustained activation of Nrf2 followed by Keap1 inactivation leads cancer cells to growth, proliferation, angiogenesis, and resistance to chemo-radiotherapies (11-14).

Here, we first investigated the effects of AAVC-I on OSCC cells using the HSC-3 cell line as a model, and then examined the effects of AAVC-I on the Keap1/Nrf2 signaling pathway. Then, this study explored the mechanism of AAVC-I -induced apoptosis in cells derived from OSCCs, which could be helpful in developing new chemotherapeutics for treating patients with OSCCs. We present this article in accordance with the MDAR reporting checklist (available at https://tcr.amegroups.com/article/view/10.21037/tcr-24-182/rc).

Highlight box

Key findings

- In this study, we observed that *Agkistrodon acutus* venom component I (AAVC-I) induces apoptosis in oral squamous cell carcinoma (OSCC) cells (HSC-3) and modulates oxidative stress levels through the Keap1/Nrf2 signaling pathway.

What is known and what is new?

- Although previous studies have found that AAVC-I can induce apoptosis of cancer cells, the specific mechanism has remained unknown.
- In this study, we elucidated that AAVC-I induces apoptosis through the endogenous pathway, providing a deeper exploration of its underlying mechanism.

What is the implication, and what should change now?

- Our study identifies AAVC-I as a potential therapeutic drug for OSCC with the capacity to overcome drug resistance. However, further exploration is needed to fully understand the related mechanisms.

Methods

Isolation and purification of AAVC-I

The venom of *Agkistrodon acutus* was procured from the Qimen Snakebite Research Institute (Huangshan, China). The lyophilized venom from *Agkistrodon acutus* was dissolved in a 5 mM sodium phosphate buffer (pH 8.0) and then centrifuged at 10,000 g for 15 minutes at 4 ℃. The supernatant was loaded into a DE-52 ion exchange chromatography column and equilibrated with the same 5 mM sodium phosphate buffer solution (pH 8.0). Gradient elution was performed using the same sodium phosphate buffer solution and 1 mol/L NaCl, with a flow rate set at 1.5 mL/min. Following desalting and dehydration, the fraction (peak I) was collected (*Figure 1*).

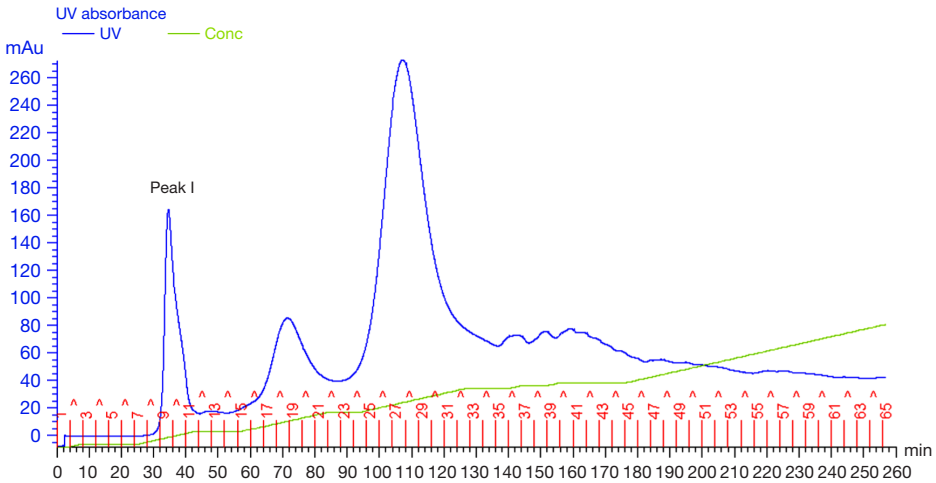

Figure 1 Results of using DEAE-cellulose column chromatography to separate the components of *Agkistrodon acutus* venom. Conc means the concentration of buffer solution; it will rise over time and eventually reach 1 mol/L. The red numbers on the horizontal axis represent the fraction numbers. UV, ultraviolet; mAu, milli-absorbance unit.

Cell culture and treatment

The Tongji Medical College of Huazhong University of Science and Technology provided the HSC-3 cells for the study. The cells were stored in the Central Laboratory of the First Affiliated Hospital of Wannan Medical College until use. They were grown on the 90% minimum essential medium (MEM) plus 10% fetal bovine serum (FBS) and 1% double antibiotic (penicillin/streptomycin), and were cultured under 5% CO_2, 37 ℃ constant temperature, and humidity conditions. When the cell growth reached the logarithmic phase, they were sub-cultured at a ratio of 1:4 and were used for subsequent experiments.

First, treatment of AAVC-I at different concentrations (0, 0.25, 0.5, 1, 2, 4, 8, 12, 16 μg/mL) were set up for cytotoxicity experiments. Based on the results of the cytotoxicity experiments, the concentrations for subsequent experiments were selected.

Cytotoxicity test

HSC-3 cells were collected and seeded at a concentration of 5,000 cells per well in 96-well plates (n=5). After 12 hours of initial seeding, the cells were treated with AAVC-I at different doses and incubated for an additional 24 and 48 hours. After that, 10 μL of Cell Counting Kit-8 (CCK-8) solution (Biosharp, Hefei, China) was added to the each well and incubated for 2 hours. Then, the 96-well plate was placed on a microplate reader (BioTek, Winooski, VT, USA) and measured the absorbance at 450 nm. Finally, the cell survival rates were calculated as follows: average optical density (OD) value of drug treatment group/average OD value of control group × 100%.

Detection of apoptosis and mitochondrial membrane potential

HSC-3 cells were collected and seeded at a density of 2.0×10^5 cells per well in a 6-well plate. The cells were treated with different concentrations of AAVC-1 (0, 2, 4, and 8 μg/mL) after 12 hours of initial seeding. Apoptosis of cells following the treatment was analyzed using Annexin V-FITC kit (Servicebio, Wuhan, China) by a flow cytometry (Beckman Coulter, Brea, CA, USA). The mitochondrial membrane potential of treated and untreated cells was examined with a flow cytometry and a fluorescent microplate reader followed by staining the cells with mitochondrial membrane potential detection kit (JC-1) (Beyotime, Haimen, China) according to the manufacturers' guidelines.

Western blot

After treatment of HSC-3 cells at various doses of AAVC-I for 12 hours, cells were collected and washed with phosphate-buffered saline (PBS) 3 times. Then, the cytosolic and nuclear proteins were collected according to the instructions of nuclear and cytoplasmic proteins extraction

kits (Beyotime). The total proteins were collected using Western and IP Cell Lysis Buffer (Beyotime) containing 1 mM protease inhibitor. A bicinchoninic acid (BCA) kit (Beyotime) was used to determine the concentration of protein. After that, 30 μg of protein was loaded into each well of 6%, 10%, and 15% sodium dodecyl sulfate polyacrylamide gel electrophoresis (SDS-PAGE) to separate the proteins and then transferred to polyvinylidene fluoride (PVDF) membranes. The membranes were then incubated with Bax (Beyotime), Bcl2 (Santa Cruz Biotechnology, Santa Cruz, CA, USA), caspase-3 (Wanleibio, Shenyang, China), cleaved caspase-3 (Wanleibio), caspase-9 (Wanleibio), cleaved caspase-9 (Wanleibio), Cyt-c (Servicebio), Keap1 (Servicebio), Nrf2 (Servicebio), HO-1 (Servicebio), NQO1 (Servicebio), β-actin (Servicebio), and Lamin-b (Wanleibio) antibodies overnight at 4 ℃. Afterwards, they were washed with PBS with Tween 20 (PBST) for 30 minutes and then incubated with horseradish peroxidase (HRP) coupled secondary antibody for 1 hour at room temperature. Finally, the signals of the target proteins were detected using an enhanced chemiluminescence (ECL) detection system, and the grayscale values of the target proteins bands were analyzed using Image J software version 1.8.0 (National Institutes of Health, Bethesda, MD, USA). β-actin was used as the total proteins, and Lamin-b was used as the nuclear proteins loading controls.

Detection of oxidative stress

HSC-3 cells were seeded at a density of 2.0×10^5 cells per well in 6-well plates. After 12 hours of seeding, cells were treated with different concentrations (0, 2, 4, 8 μg/mL) of AAVC-I for an additional 12 hours. For the estimation of ROS, DCFH-DA (Jiancheng Bioengineering Institute, Nanjing, China) and Bodipy-C11 (Maokang Biotechnology, Shanghai, China) fluorescent probes were used. In short, the cells were incubated with the probes for 30 minutes followed by removal of treatment and the ROS levels were measured according to the instructions using flow cytometry and fluorescence microscope.

Measurement of glutathione (GSH), superoxide dismutase (SOD), and malondialdehyde (MDA) was performed according to the reagent kits (Wanleibio). For this experiment, samples were collected from HSC-3 cells and the protein concentration of the samples were determined using the BCA assay kit and the activity of SOD, GSH, and MDA were measured according to the manufacturer's guidelines.

Statistical analysis

All experiments were carried out independently at least 3 times. Statistical analysis was performed using SPSS 18.0 statistical software (IBM Corp., Armonk, NY, USA). Measurement data were expressed as $\bar{x} \pm s$, and *t*-tests were used for comparison between two groups. Analysis of variance (ANOVA) was used for multiple group comparisons. A P value <0.05 was considered a significant difference.

Results

Cytotoxicity and apoptosis

The effects of AAVC-I on the survival rates of HSC-3 cells are presented in *Figure 2A*. AAVC-I induced HSC-3 cell death in a concentration-dependent manner with a 50% inhibiting concentration (IC_{50}) of 8.86 μg/mL after 24 hours of treatment. It was noted that at 2 μg/mL of AAVC-I, the survival rates of HSC-3 cells started to decrease notably, and at a concentration of 4 μg/mL, it reached a statistically significant difference. Therefore, in subsequent experiments, the treatment groups were used as follows: 2, 4, and 8 μg/mL as low, medium, and high concentration groups, respectively (*Table 1*).

The treatment of AAVC-I induced apoptosis of HSC-3 cells (*Figure 2B*) and the proportion of apoptotic and necrotic cells were increased with the increment of AAVC-I concentration.

AAVC-I induced reduction of mitochondrial membrane potential

Reduction of mitochondrial membrane potential is a hallmark of apoptosis. Thus, we used a JC-1 kit to measure the mitochondrial membrane potential of HSC-3 cells followed by AAVC-I treatment. It was noted that AAVC-I caused a significant reduction of mitochondrial membrane potential of HSC-3 cells (*Figure 3*). Interestingly, with the increasing of AAVC-I concentration, the intensity of red fluorescence decreased, whereas the intensity of green fluorescence increased. These results indicated the higher loss of mitochondrial membrane potential with higher doses of AAVC-I treatment (*Figure 3*).

Regulation of apoptosis-related proteins by AAVC-I treatment

The upregulation or downregulation of apoptosis-related

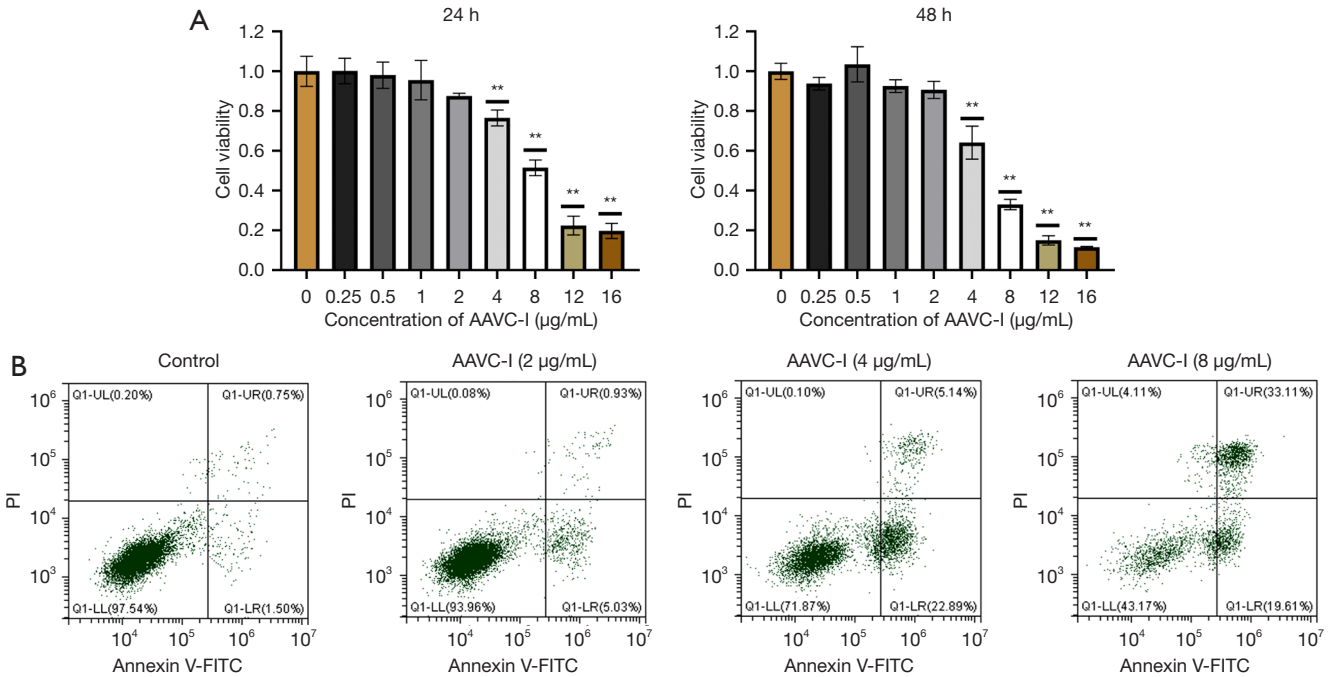

Figure 2 Effect of AAVC-I on the survival rate and apoptosis of HSC-3 cells. (A) Changes in survival rate of HSC-3 cells treated with different concentrations of AAVC-I. **, compared with the control group, P<0.01. (B) Apoptosis of HSC-3 cells treated with AAVC-I. AAVC-I, *Agkistrodon acutus* venom component I; Q1, the selected cell range; UL, upper left quadrant; UR, upper right quadrant; LL, lower left quadrant; LR, lower right quadrant; PI, propidium iodide; FITC, fluorescein isothiocyanate.

Table 1 Effect of AAVC-I on the growth of HSC-3 cells

Group	Cell viability (24 h)	Cell viability (48 h)
Control	1.000±0.076	1.000±0.040
AAVC-I		
0.25 μg/mL	1.001±0.064	0.938±0.032
0.5 μg/mL	0.980±0.066	1.035±0.089
1 μg/mL	0.955±0.099	0.925±0.032
2 μg/mL	0.876±0.014	0.907±0.043
4 μg/mL	0.765±0.040	0.641±0.083
8 μg/mL	0.515±0.039	0.331±0.026
12 μg/mL	0.225±0.047	0.150±0.024
16 μg/mL	0.197±0.038	0.116±0.004

Data are presented as mean ± standard deviation. AAVC-I, *Agkistrodon acutus* venom component I.

proteins in HSC-3 cells followed by AAVC-I were analyzed using western blots. The expressions of Bax, Bcl2, caspase-3, cleaved caspase-3, caspase-9, cleaved caspase-9, and Cyt-c were examined. It was found that with the increasing of AAVC-I concentrations, the expression levels of Bax, cleaved caspase-3, cleaved caspase-9, and Cyt-c increased whereas the expression level of Bcl2 decreased significantly (P<0.05). The expression of caspase-3 at various doses remained the same whereas caspase-9 expression increased significantly at 4 μg/mL or higher doses of AAVC-I treatment (*Figure 4*).

Inactivation of the Keap1/Nrf2 pathway by AAVC-I treatment

The expression levels of Keap1, Nrf2, HO-1, NQO1, and Nrf2 in the nuclear proteins were examined. The expression of Keap1 increased significantly with increasing concentrations of AAVC-I, whereas the expression of Nrf2 decreased in the nuclear proteins fraction (*Figure 5*). However, the expression of Nrf2 in total proteins did not change significantly. In addition, expression of heme oxygenase 1 (HO-1) slightly increased at low concentrations (2 μg/mL) yet decreased significantly at the concentrations of 4 μg/mL or higher doses. Furthermore, the expression of

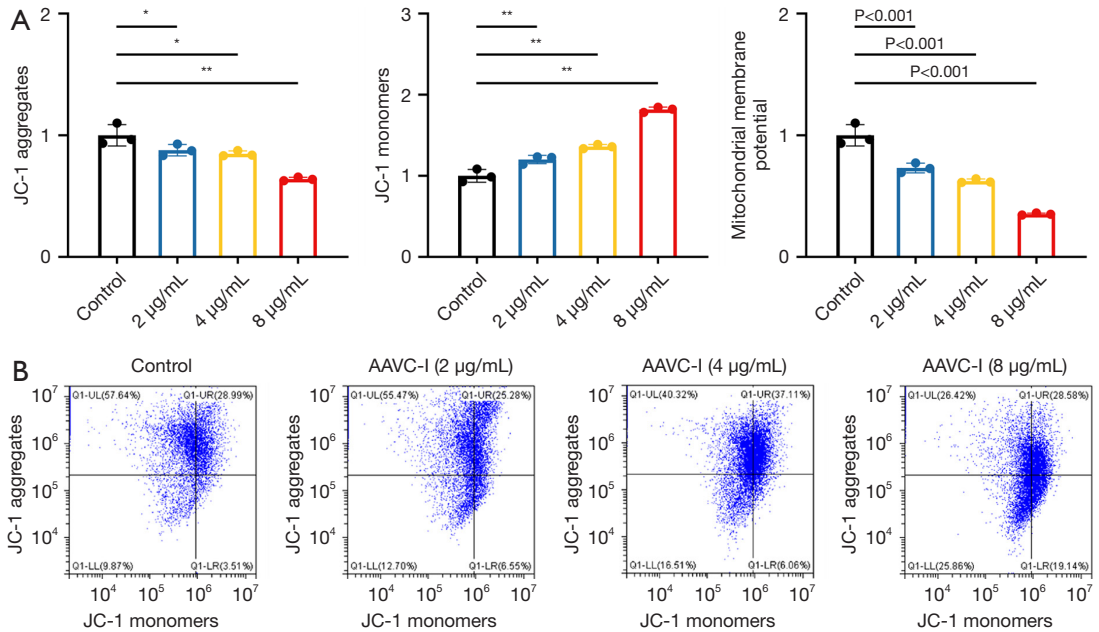

Figure 3 Mitochondrial membrane potential of HSC-3 cells treated with AAVC-I. (A) Fluorescent microplate reader; (B) flow cytometry. *, compared with the control group, P<0.05; **, compared with the control group, P<0.01. AAVC-I, *Agkistrodon acutus* venom component I; Q1 represents the selected cell range. UL, upper left quadrants; UR, upper right quadrants; LL, lower left quadrants.

NAD(P)H:quinone oxidoreductase 1 (NQO1) significantly increased at low (2 μg/mL) and medium (4 μg/mL) concentrations, and on the contrary, it decreased at high concentrations (8 μg/mL). However, this reduction of NQO1 at higher doses of AAVC-I treatment did not reach the statistical significance level (*Figure 5*). These results implied that treatment of HSC-3 cells with AAVC-I induced inactivation of Keap1/Nrf2 signaling pathway.

Induction of oxidative stress in HSC-3 cells by AAVC-I treatment

Production of ROS in HSC-3 cells after AAVC-I treatment at low, medium, and high concentrations is presented in *Figure 6*. The results showed that ROS level in HSC-3 cells increased significantly after AAVC-I treatment with a concentration-dependent manner (*Figures 6,7*). In addition, analysis of GSH and SOD showed that at lower dose (2 μg/mL) of AAVC-I, the level of GSH and SOD increased slightly, whereas it significantly decreased at high concentration of AAVC-I (8 μg/mL) treatment (*Figure 8A,8B*). Meanwhile, the level of MDA in HSC-3 cells increased with the increment of AAVC-I treatment, indicating a concentration-dependent pattern of elevation of MDA in HSC-3 cells receiving AAVC-I treatment (*Figure 8C*).

Discussion

Chemotherapy is an important option for the patients with OSCC in clinical settings. However, low response, adverse side effects, and resistance to the chemotherapies deteriorate the quality of life and limit their point-of-care application. Thus, it is an urgent need to develop effective drugs for the treatment of patients with OSCC. The present study revealed that AAVC-I inhibited the survival of OSCC (HSC-3) cells significantly through induction of the apoptosis of cancer cells. Also, it was noted that AAVC-I reduced the mitochondrial membrane potential and increased the ROS levels in HSC-3 cells. In addition, AAVC-I may regulate the Keap1/Nrf2 signaling pathway to increase oxidative stress levels in OSCC cells, resulting in effective elimination of cancer cells (*Figure 9*).

Snake venom is a complex mixture of proteins and peptides that exhibit biological activity during physiological processes. Therefore, further separation and detailed study of the components within this mixture is currently a research hotspot. Previous studies (15-17) have highlighted the potential applications of snake venom toxins in

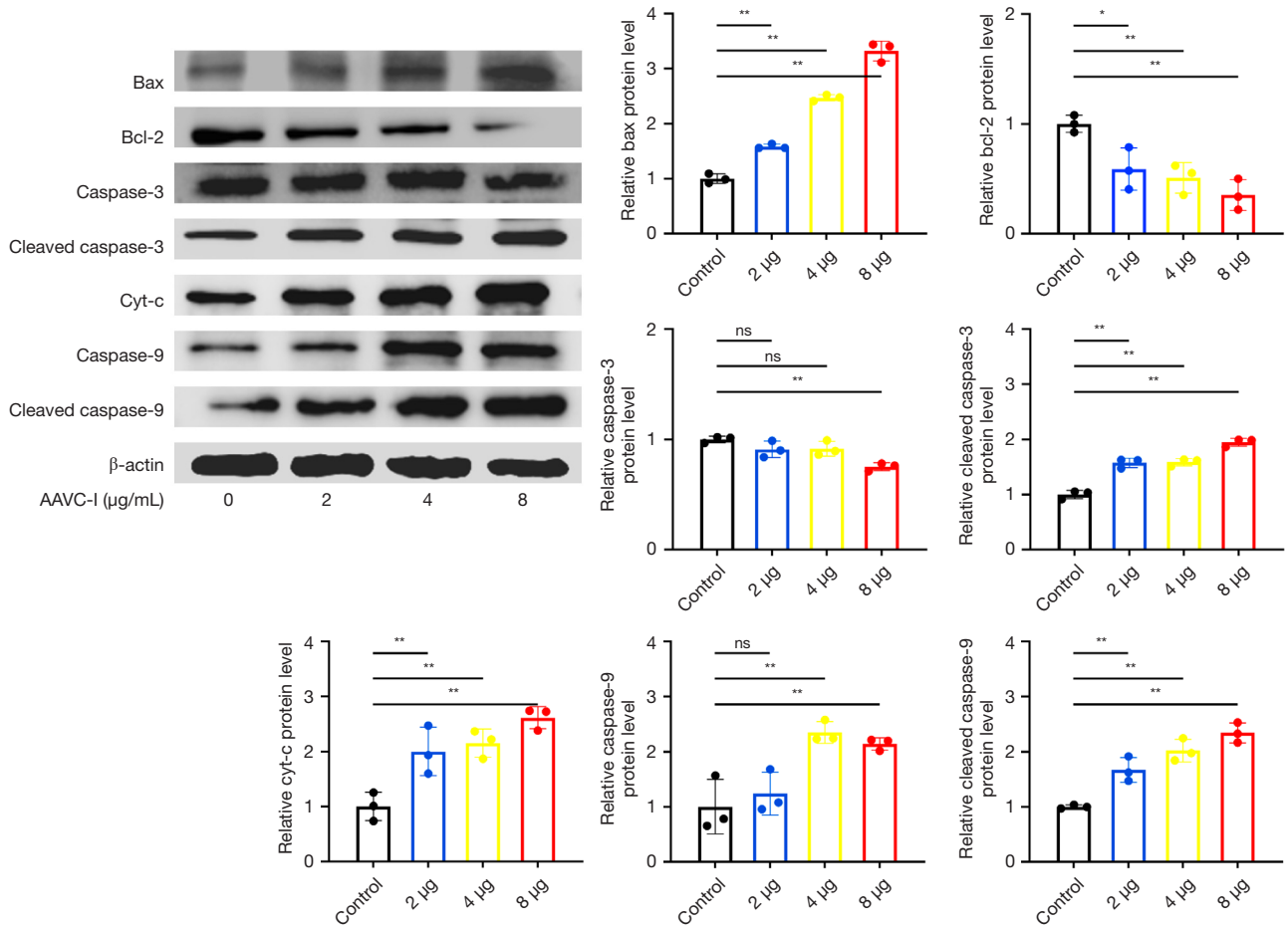

Figure 4 Effect of AAVC-I on the expression of apoptosis related proteins in HSC-3 cells. *, compared with the control group, P<0.05; **, compared with the control group, P<0.01; ns, compared with the control group, there was no significant difference. AAVC-I, *Agkistrodon acutus* venom component I.

anti-tumor therapy. Ha *et al.* identified four proteins: PLA2, SVMP, CRiSP, and CTL/snalec in the venom of *Agkistrodon acutus* using methods such as mass spectrometry, electrophoresis, and N-terminal sequencing (16). Among these, PLA2 has been suggested to exhibit anti-tumor and angiogenic effects, although some reports (17,18) indicate that PLA2 lacks cytotoxicity. SVMP has been documented in multiple studies (15,16) as disrupting the extracellular matrix, altering the adhesion and migration of cancer cells, and has significant implications for the development of anticancer drugs. CRiSP has been recognized for biological functions such as antimicrobial activity and Ca^{2+} and K^{+} channel blockade, but its anti-tumor activity has yet to be reported (19). AAVC-I, an anti-tumor component extracted from the crude venom of *Agkistrodon acutus*, may enhance the functionality of each individual component in practical applications.

The balance between cell survival (proliferation) and death is crucial for maintaining normal growth and development. Once this balance is disrupted, it leads to the pathogenesis of cancers and other degenerative diseases. Apoptosis, a key programmed cell death phenomenon, is often considered an effective target for developing cancer therapeutics (20). In this study, considerable portion of cells treated with AAVC-I underwent apoptosis, thereby reducing the survival rate of HSC-3 cells in a dose-dependent manner. Similarly, AAVC-I causes reduction of growth and proliferation of cancer cells derived from laryngeal, lung, and other types of cancers (7,8). Additionally, at a higher dose (8 μg/mL), AAVC-I increased the proportion of necrotic cells along with an increase in the proportion of apoptotic cell populations.

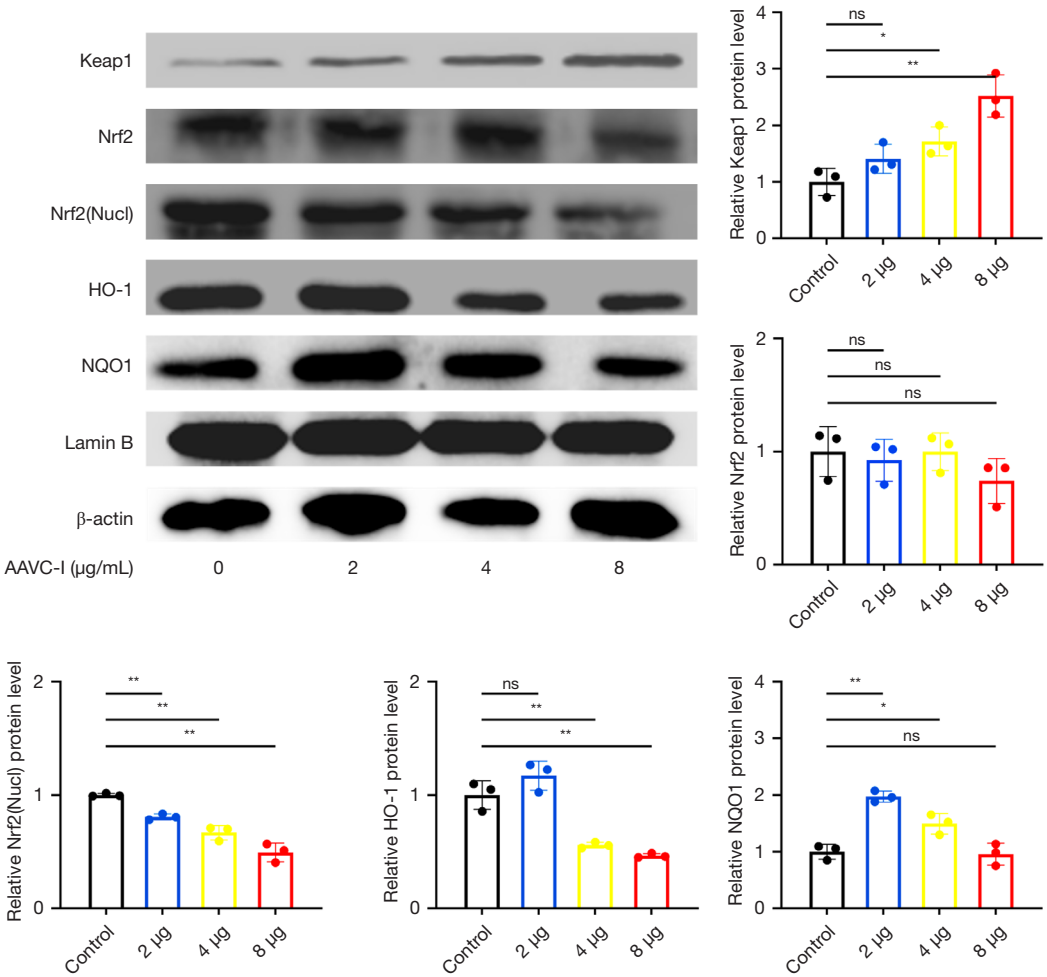

Figure 5 Expression of oxidative stress pathway proteins in HSC-3 cells. *, compared with the control group, P<0.05; **, compared with the control group, P<0.01; ns, compared with the control group, there was no significant difference. AAVC-I, *Agkistrodon acutus* venom component I.

Apoptosis is a type of programmed cell death mediated by various pathways, including exogenous (death receptors) and endogenous (mitochondria), ultimately leading to cell death. Related molecular events include changes in mitochondrial membrane potential, DNA breakage, and specific protease cascades. In this process, Bcl2, by binding to BH3, promotes the formation of pro-apoptotic effectors by interacting with Bax and Bak. This complex affects mitochondrial membrane permeability and releases Cyt-c into the cytoplasm. Subsequently, Cyt-c binds to Apaf-1, resulting in the formation of an apoptotic body, which triggers the caspase cascade reactions of apoptosis (21,22). Cyt-c is translocated to the cytoplasm, oxidative phosphorylation is decoupled, and higher levels of ROS such as H_2O_2, and OH– are generated (23). This excessive ROS generation and accumulation induce apoptosis of cells through the mitochondrial and endoplasmic reticulum pathways (24,25). AAVC-I treatment of HSC-3 cells caused a reduction in the anti-apoptotic protein Bcl2 and increased the expression of the pro-apoptotic protein Bax, which is consistent with a previous study on oropharyngeal cancer (7). Additionally, HSC-3 cells receiving AAVC-I showed a decrease in mitochondrial membrane potential and an increase in ROS levels. Next, we further examined the expression of cleaved caspase-9 and caspase-3, and noted that the expression of cleaved caspase-9 and cleaved caspase-3 significantly increased after AAVC-I treatment. Therefore, AAVC-I primarily induces cell apoptosis

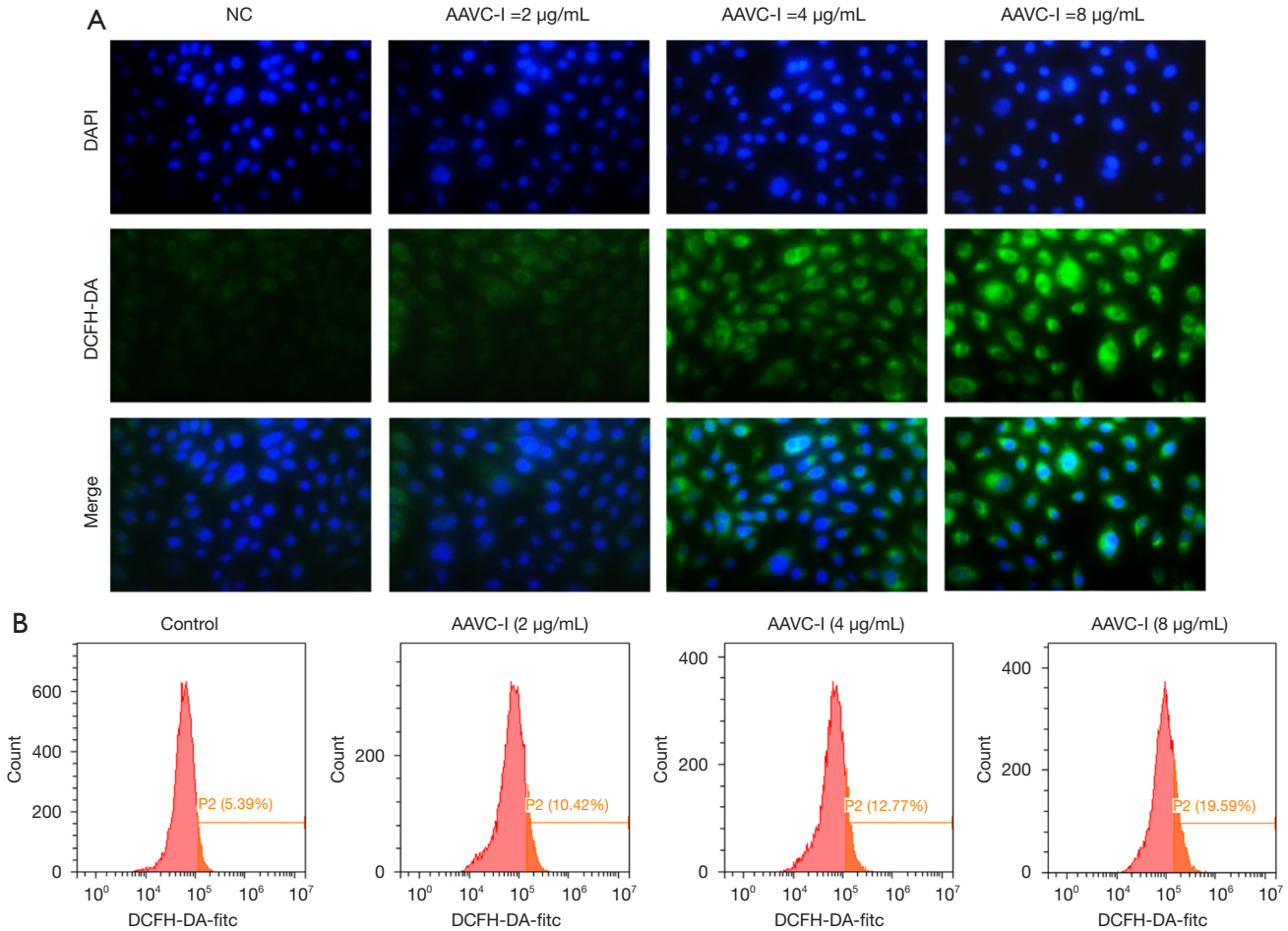

Figure 6 ROS levels in HSC-3 cells. After treatment of HSC-3 cells with different concentrations of AAVC-I, the production of ROS was detected by DCFH-DA probe. (A) Fluorescence staining; green: the production of ROS in HSC-3 cells; blue: nucleus. Magnification: 400×. (B) ROS levels in HSC-3 cells detected by flow cytometry. NC, control group; AAVC-I, *Agkistrodon acutus* venom component I; DAPI, 4',6-diamidino-2-phenylindole; ROS, reactive oxygen species.

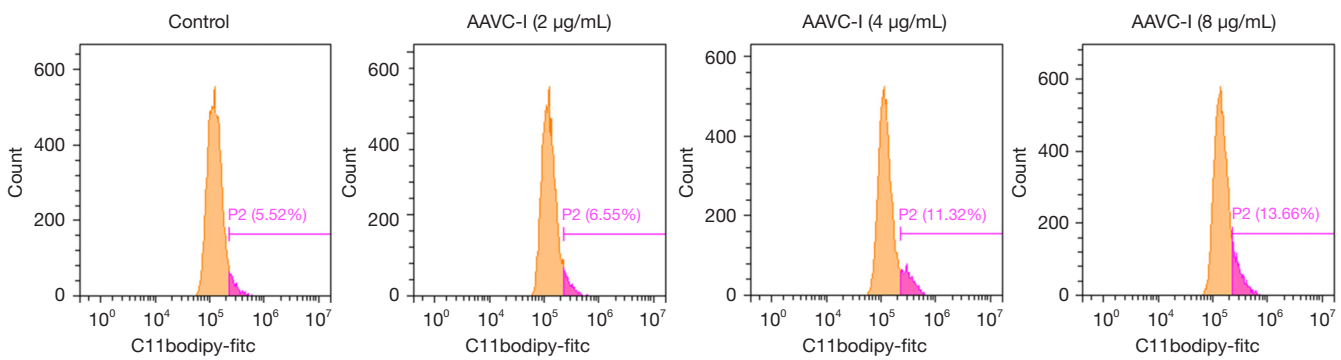

Figure 7 Lipid ROS levels in HSC-3 cells. AAVC-I, *Agkistrodon acutus* venom component I; ROS, reactive oxygen species.

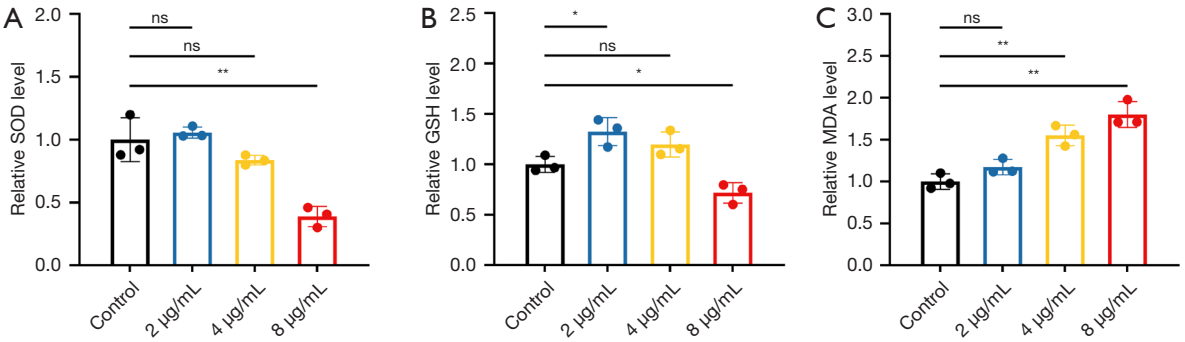

Figure 8 SOD, GSH, and MDA levels in HSC-3 cells. (A) SOD; (B) GSH; (C) MDA. *, compared with the control group, P<0.05; **, compared with the control group, P<0.01; ns, compared with the control group, there was no significant difference. SOD, superoxide dismutase; GSH, glutathione; MDA, malondialdehyde.

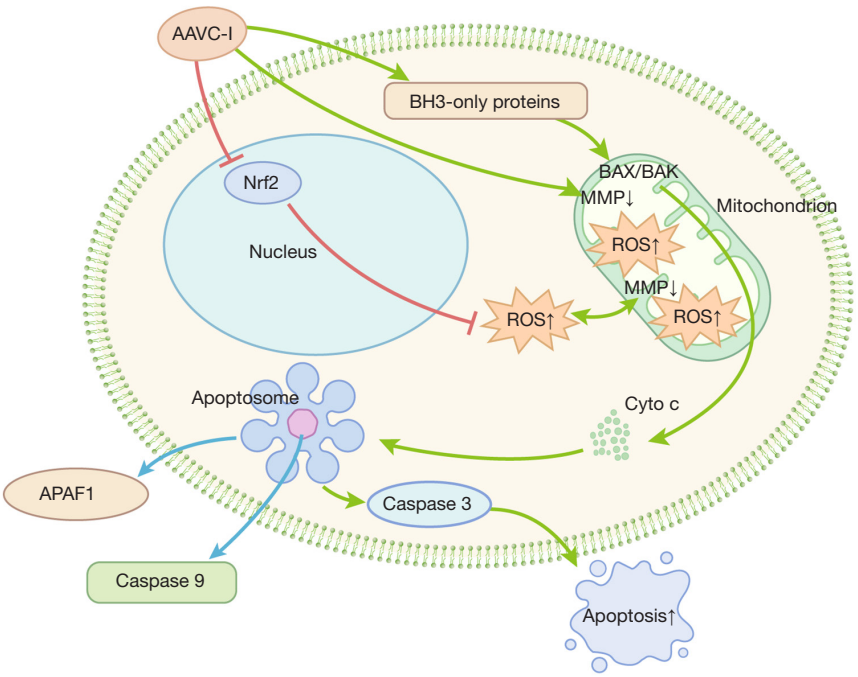

Figure 9 Possible mechanism of AAVC-I. AAVC-I induces apoptosis in HSC-3 cells through the classical mitochondrial pathway and enhances cellular oxidative stress levels by inhibiting the expression of Nrf2 in the nucleus. Green arrows represent a promoting effect on the next stage, red arrows represent the inhibitory effect, black arrows indicate an increase in expression level. Blue arrows mark the composition of the apoptotic complex (this figure was drawn by Adobe Illustrator). AAVC-I, *Agkistrodon acutus* venom component I; ROS, reactive oxygen species; MMP, mitochondrial membrane potential.

through endogenous pathways.

ROS accumulation in cancer cells can induce oxidative stress by modulating the activity of the Keap1/Nrf2 signaling pathway. Activation of Nrf2 promotes an antioxidant response and reduces intracellular ROS levels. Meanwhile, inactivation of Nrf2 is associated with reduced cell proliferation. Therefore, Nrf2 can promote oncogene-induced cancer growth and proliferation (26-28). Results from the present study suggest that AAVC-I appears to be a potential inhibitor of Nrf2, as the expression of Nrf2 in both total and nuclear proteins of HSC-3 cells decreased significantly after AAVC-I treatment. Most importantly,

Nrf2 expression in the nucleus was inhibited even at low concentrations of AAVC-I (2 μg/mL). Under physiological conditions, Keap1 binds to Nrf2 and localizes it in the cytoplasm, resulting in its ubiquitination and degradation. However, under oxidative stress, Nrf2 dissociates from Keap1 and translocates to the nucleus, where it interacts with the antioxidant response element (ARE), leading to the activation of transcription of a series of antioxidant response genes, thereby enhancing the cell's antioxidant capacity (28). AAVC-I treatment induced excessive ROS generation and simultaneously reduced Nrf2 expression and upregulated Keap1 expression. Deng *et al.* recently reported that metformin can inhibit the Nrf2/HO-1 signaling pathway and increase oxidative stress levels in cancer cells. When oxidative stress levels in cells rise, MDA levels typically increase, whereas those of SOD and GSH decrease (29). This aligns with our research findings, which indicate that AAVC-I elevates oxidative stress levels in HSC-3 cells. In an earlier study, Park *et al.* found that viper venom can elevate oxidative stress levels in neuroblastoma cells; however, they only measured two indicators of oxidative stress, ROS and mitochondrial membrane potential, and their evaluation of the corresponding molecular events was incomplete (30). Thus, the Keap1/Nrf2 signaling pathway is the main antioxidant pathway in cells, and interference with this pathway by AAVC-I appears promising for developing better therapeutics. Interestingly, this finding contrasts with traditional chemotherapy drugs such as cisplatin, which increases the expression of Nrf2 in cancer cells, thereby leading to drug resistance (31,32). Furthermore, AAVC-I treatment induced the downregulation of HO-1 in HSC-3 cells, whereas NQO1 expression was mildly upregulated. It has been observed that overexpression of HO-1 and NQO1 is associated with drug resistance in cancer cells (31,32). However, overexpression of NQO1 alone does not affect the Keap1/Nrf2 pathway (33,34).

In this study, we primarily report that AAVC-I, a mixture isolated from *Agkistrodon acutus* venom, may regulate the oxidative stress pathway and induce tumor cell apoptosis. Considering the significant side effects of existing chemotherapy drugs, the extraction of anti-tumor agents from snake venom may offer new breakthroughs in future cancer treatment. However, our current research is limited to a single cell line *in vitro* and the lack of *in vivo* evidence; additionally, the biological safety of AAVC-I has not been evaluated. These aspects need to be addressed in subsequent studies.

Conclusions

In summary, this study demonstrates that AAVC-I inhibits the proliferation and survival of OSCC (HSC-3) cells by inducing the endogenous apoptosis pathway. Unlike traditional chemotherapy drugs, AAVC-I not only increases oxidative stress but also inhibits the Keap1/Nrf2 signaling pathway, potentially overcoming drug resistance caused by activation of this pathway. Under oxidative stress conditions, Nrf2 translocates to the nucleus and activates the transcription of a series of antioxidant genes, thereby mitigating the oxidative stress response. AAVC-I may inhibit this process by promoting ubiquitin-mediated degradation of Nrf2 in the cytoplasm. However, further studies involving animal models and the examination of AAVC-I's biological safety *in vivo* and its host toxicity are required. Additionally, as only one cell line was used in this study, more research is necessary to support AAVC-I as a new therapeutic for treating oral cancer.

Acknowledgments

Funding: This study was supported by the Applied Basic Research Project of Wuhu Science and Technology Bureau (No. 2022jc68), Open Project of Anhui Provincial Key Laboratory for Active Biomacromolecules (No. LAB202206), Young and Middle-Aged Scientific Research Fund from Wannan Medical College (No. WK202202, No. WK2023ZQNZ41), and Major Scientific Research Project of Anhui Provincial Department of Education (No. KJ2021ZD0103).

Footnote

Reporting Checklist: The authors have completed the MDAR reporting checklist. Available at https://tcr.amegroups.com/article/view/10.21037/tcr-24-182/rc

Data Sharing Statement: Available at https://tcr.amegroups.com/article/view/10.21037/tcr-24-182/dss

Peer Review File: Available at https://tcr.amegroups.com/article/view/10.21037/tcr-24-182/prf

Conflicts of Interest: All authors have completed the ICMJE uniform disclosure form (available at https://tcr.amegroups.com/article/view/10.21037/tcr-24-182/coif). The authors have no conflicts of interest to declare.

Ethical Statement: The authors are accountable for all aspects of the work in ensuring that questions related to the accuracy or integrity of any part of the work are appropriately investigated and resolved.

References

1. Bray F, Ferlay J, Soerjomataram I, et al. Global cancer statistics 2018: GLOBOCAN estimates of incidence and mortality worldwide for 36 cancers in 185 countries. CA Cancer J Clin 2018;68:394-424.
2. Siegel RL, Miller KD, Fuchs HE, et al. Cancer statistics, 2022. CA Cancer J Clin 2022;72:7-33.
3. Neville BW, Day TA. Oral cancer and precancerous lesions. CA Cancer J Clin 2002;52:195-215.
4. He K, Liu X, Hoffman RD, et al. G-CSF/GM-CSF-induced hematopoietic dysregulation in the progression of solid tumors. FEBS Open Bio 2022;12:1268-85.
5. Waheed H, Moin SF, Choudhary MI. Snake Venom: From Deadly Toxins to Life-saving Therapeutics. Curr Med Chem 2017;24:1874-91.
6. Koh CY, Kini RM. From snake venom toxins to therapeutics--cardiovascular examples. Toxicon 2012;59:497-506.
7. Chai L, Huang T, Wang Z, et al. AAVC-I promotes apoptosis of human oral squamous cell carcinoma through the mitochondrial pathway. Int J Clin Exp Pathol 2019;12:3968-74.
8. Xu P, Zhang GB, Wang F, et al. Inhibitory effect of anti-tumor componentIfrom Agkistrodon acutus venom on human lung cancer A549 cells. Chinese Journal of Clinical Pharmacology and Therapeutics 2014;19:493-6.
9. Sun Y, Bao PJ, Zhang GB. Purification and characterization of Protein C activator from Agkistrodon acutus Venom. Prep Biochem Biotechnol 2020;50:907-14.
10. Xu F, Xu J, Xiong X, et al. Salidroside inhibits MAPK, NF-κB, and STAT3 pathways in psoriasis-associated oxidative stress via SIRT1 activation. Redox Rep 2019;24:70-4.
11. Hafez AM, Harb OA, Alattar AZ, et al. Clinico-pathological and prognostic implications of Srx, Nrf2, and PROX1 expression in gastric cancer and adjacent non-neoplastic mucosa - an immunohistochemical study. Contemp Oncol (Pozn) 2020;24:229-40.
12. Cuadrado A, Rojo AI, Wells G, et al. Therapeutic targeting of the NRF2 and KEAP1 partnership in chronic diseases. Nat Rev Drug Discov 2019;18:295-317.
13. Zhao Y, Wang Y, Zhang M, et al. Protective Effects of Ginsenosides (20R)-Rg3 on H(2) O(2) -Induced Myocardial Cell Injury by Activating Keap-1/Nrf2/HO-1 Signaling Pathway. Chem Biodivers 2021;18:e2001007.
14. Singh A, Daemen A, Nickles D, et al. NRF2 Activation Promotes Aggressive Lung Cancer and Associates with Poor Clinical Outcomes. Clin Cancer Res 2021;27:877-88.
15. Marinho AD, Lucena da Silva E, Jullyanne de Sousa Portilho A, et al. Three snake venoms from Bothrops genus induced apoptosis and cell cycle arrest in K562 human leukemic cell line. Toxicon 2024;238:107547.
16. Ha SJ, Choi YO, Kwag EB, et al. Qualitative Analysis of Proteins in Two Snake Venoms, Gloydius Blomhoffii and Agkistrodon Acutus. J Pharmacopuncture 2022;25:52-62.
17. Hiu JJ, Yap MKK. Cytotoxicity of snake venom enzymatic toxins: phospholipase A2 and l-amino acid oxidase. Biochem Soc Trans 2020;48:719-31.
18. Calderon LA, Sobrinho JC, Zaqueo KD, et al. Antitumoral activity of snake venom proteins: new trends in cancer therapy. Biomed Res Int 2014;2014:203639.
19. Sunagar K, Johnson WE, O'Brien SJ, et al. Evolution of CRISPs associated with toxicoferan-reptilian venom and mammalian reproduction. Mol Biol Evol 2012;29:1807-22.
20. Wu R, Zuo W, Xu X, et al. MCU That Is Transcriptionally Regulated by Nrf2 Augments Malignant Biological Behaviors in Oral Squamous Cell Carcinoma Cells. Biomed Res Int 2021;2021:6650791.
21. Radha G, Raghavan SC. BCL2: A promising cancer therapeutic target. Biochim Biophys Acta Rev Cancer 2017;1868:309-14.
22. Kaloni D, Diepstraten ST, Strasser A, et al. BCL-2 protein family: attractive targets for cancer therapy. Apoptosis 2023;28:20-38.
23. Sinha K, Das J, Pal PB, et al. Oxidative stress: the mitochondria-dependent and mitochondria-independent pathways of apoptosis. Arch Toxicol 2013;87:1157-80.
24. Sun W, Ni Z, Li R, et al. Flurochloridone induces Sertoli cell apoptosis through ROS-dependent mitochondrial pathway. Ecotoxicol Environ Saf 2021. [Epub ahead of print]. doi: 10.1016/j.ecoenv.2021.112183.

25. Zhang F, Ni Z, Zhao S, et al. Flurochloridone Induced Cell Apoptosis via ER Stress and eIF2α-ATF4/ATF6-CHOP-Bim/Bax Signaling Pathways in Mouse TM4 Sertoli Cells. Int J Environ Res Public Health 2022;19:4564.
26. DeNicola GM, Karreth FA, Humpton TJ, et al. Oncogene-induced Nrf2 transcription promotes ROS detoxification and tumorigenesis. Nature 2011;475:106-9.
27. Li Z, Mo RL, Gong JF, et al. Dihydrotanshinone I inhibits gallbladder cancer growth by targeting the Keap1-Nrf2 signaling pathway and Nrf2 phosphorylation. Phytomedicine 2024;129:155661.
28. Mukherjee AG, Gopalakrishnan AV. The mechanistic insights of the antioxidant Keap1-Nrf2 pathway in oncogenesis: a deadly scenario. Med Oncol 2023;40:248.
29. Deng C, Xiong L, Chen Y, et al. Metformin induces ferroptosis through the Nrf2/HO-1 signaling in lung cancer. BMC Pulm Med 2023;23:360.
30. Park MH, Son DJ, Kwak DH, et al. Snake venom toxin inhibits cell growth through induction of apoptosis in neuroblastoma cells. Arch Pharm Res 2009;32:1545-54.
31. Aboulkassim T, Tian X, Liu Q, et al. A NRF2 inhibitor selectively sensitizes KEAP1 mutant tumor cells to cisplatin and gefitinib by restoring NRF2-inhibitory function of KEAP1 mutants. Cell Rep 2023;42:113104.
32. Liang C, Zhang HY, Wang YQ, et al. TMED2 Induces Cisplatin Resistance in Breast Cancer via Targeting the KEAP1-Nrf2 Pathway. Curr Med Sci 2023;43:1023-32.
33. Wu YL, Wang D, Peng XE, et al. Epigenetic silencing of NAD(P)H:quinone oxidoreductase 1 by hepatitis B virus X protein increases mitochondrial injury and cellular susceptibility to oxidative stress in hepatoma cells. Free Radic Biol Med 2013;65:632-44.
34. Takei K, Hashimoto-Hachiya A, Takahara M, et al. Cynaropicrin attenuates UVB-induced oxidative stress via the AhR-Nrf2-Nqo1 pathway. Toxicol Lett 2015;234:74-80.

Cite this article as: Tao T, Zhang F, Chai L, Xing X, Wan C, Tao Z, Wang Z. Effect of *Agkistrodon acutus* venom (AAVC-I) on apoptosis through modulation of the Keap1/Nrf2 pathway in HSC-3 oral squamous cell carcinoma cells. Transl Cancer Res 2024;13(8):4341-4353. doi: 10.21037/tcr-24-182

